
Using the Dynamic Energy Budget theory to evaluate the bioremediation potential of the polychaete *Hediste diversicolor* in an integrated multi-trophic aquaculture system

Lopes Galasso Helena ^{1,2,*}, Lefebvre Sebastien ³, Aliaume Catherine ⁴, Sadoul Bastien ¹,
Callier Myriam ^{1,*}

¹ MARBEC, Univ Montpellier, CNRS, Ifremer, IRD, Palavas-les-Flots, France

² CAPES Foundation, Ministry of Education of Brazil, Brasília, DF 70040-020, Brazil

³ Université de Lille, Université Littoral Côte d'Opale, CNRS, Laboratoire d'Océanologie et Géosciences (UMR 8187 LOG), Station Marine de Wimereux, F-59000 Lille, France

⁴ MARBEC, Univ Montpellier, CNRS, Ifremer, IRD, Montpellier, France

* Corresponding authors : Helena Lopes Galasso, email address : helenagalasso@gmail.com ; Myriam Callier, email address : myriam.callier@ifremer.fr

Abstract :

Integrated Multi-Trophic Aquaculture (IMTA) systems have been designed to optimize nutrient and energy use, to decrease waste, and to diversify fish-farm production. Recently, the development of detritivorous aquaculture has been encouraged, as detritivores can consume organic particulate matter, reducing benthic eutrophication and the environmental footprint of aquaculture. To this end, the polychaete *Hediste diversicolor* is a promising species due to its broad feeding behaviour and its resistance in a wide range of environments. In this study, an existing Dynamic Energy Budget (DEB) model of *H. diversicolor* was used to predict the ragworm's metabolic processes in various environmental conditions and to estimate its bioremediation capacity in an aquaculture context. First, the scaled functional response (f) was calibrated in a 98-day growth experiment with two types of food (Fish faeces and Fish feed). Then, we further validated the model using data on the ammonia excretion and oxygen consumption of individuals fed with fish faeces at four different temperatures using the previously calibrated f . Overall, we found that the DEB model was able to correctly predict the experimental data ($0.51 < \text{MRE} < 0.80$). Lastly, different environmental scenarios of seawater temperatures and assimilation rates were compared. The bioremediation potential of *H. diversicolor* was estimated based on cumulated assimilation rates, which could represent 75-289 kg of fish waste year⁻¹ for a 100 m² ragworm farm (3700 ind. m⁻²). These findings suggest that the DEB model is a promising tool for further IMTA development and management.

Highlights

► The DEB model for *Hediste diversicolor* accurately predicts metabolic processes ► Bioremediation potential of fish farm waste by *H. diversicolor* was estimated for different scenarios ► A 100 m⁻² ragworm farm could bioremediate 2-9% fish faeces produced by a 20T seabass farm per year ► DEB modelling appears to be a promising tool for further IMTA development

Keywords : DEB, Deposit feeders, Fish waste, Metabolism, Ragworm, Semelparous, Bioenergetics

44 1. Introduction

45 Fed aquaculture can impact ecosystems through the release of organic matter and
46 dissolved nutrients (Hargrave, 2005). One way to minimize aquaculture waste is to
47 develop Integrated Multi-Trophic Aquaculture (IMTA), in which organisms of different
48 trophic levels are co-cultured on the same farm (Chopin et al., 2012). This type of
49 aquaculture can include fed species (e.g. finfish or shrimp) as well as extractive species
50 such as algae that can feed on dissolved inorganic waste generated by the fed species
51 (Abreu et al., 2011; Erler et al., 2000) or filter-feeders and detritivores that can feed on
52 generated organic waste (Jiang et al., 2013; Neori et al., 2004). In open water,
53 particulate organic matter fluxes (faeces and uneaten feed) are mainly vertical (Filgueira
54 et al., 2017) and may accumulate on the bottom sediment both within the farm site and
55 close to it, inducing benthic eutrophication (Hargrave, 2005). The quantity and
56 biochemical composition of the nutrients and organic matter released depends on the
57 cultured species, the farm size, the feed composition, and the rearing conditions
58 (Brigolin et al., 2010).

59 Using detritivore species in IMTA may improve the mineralization of organic matter
60 through bioturbation processes (Hedman et al., 2011) and feeding (Cammen, 1980),
61 thus preventing benthic eutrophication. The bioremediation potential of several
62 detritivorous species has been evaluated, including fish (Katz et al., 2002; Porter et al.,
63 1996), sea cucumbers (Cubillo et al., 2016; MacDonald et al., 2013; Nelson et al., 2012;
64 Paltzat et al., 2008; Chary et al., 2020), sea urchins (Cook and Kelly, 2007; Orr et al.,
65 2014) and polychaetes (Fang et al., 2017; Marques et al., 2017). Among polychaetes,
66 *Hediste (Nereis) diversicolor* (O. F. Müller, 1776) has been widely studied (Gillet et al.,
67 2008; Mermillod-Blondin et al., 2004). Similar to other Nereididae, this species plays
68 an important ecological role by constructing burrows in sediment to create galleries.

69 Their bioturbation and ventilation activities promote nutrient fluxes between water and
70 sediment, favouring the oxygenation of the sediment (Michaud et al., 2006) and
71 enhancing organic matter mineralization and nutrient recycling (Heilskov and Holmer,
72 2001). Additionally, *H. diversicolor* can cope with a large range of environmental
73 conditions, in terms of variation in organic matter loading, temperature and salinity
74 (Kristensen, 1983; Ozoh and Jones, 1990). Moreover, its feeding behaviour is
75 diversified: it is considered a detritivore, carnivore, herbivore, suspension feeder and
76 even an optional filter feeder (Nielsen et al., 1995; Riisgård, 1994). More recently, the
77 biomitigation activity of this species has been explored (Cubillo et al., 2016; Marques et
78 al., 2017; Papaspyrou et al., 2010), and studies have demonstrated that individuals can
79 grow significantly when fed on fish waste (Bischoff et al., 2009; Wang et al. 2019).
80 Cubillo et al. (2016) and Marques et al. (2017) have also shown that *H. diversicolor*
81 could assimilate particulate organic matter from fish farms, confirming its potential for
82 IMTA. However, these studies were carried out under specific temperature and salinity
83 conditions, making predicting the bioremediation capacity in other environmental
84 conditions difficult. In this context, mechanistic models can be useful tools as they can
85 simulate physiological and ecological processes under a large range of environmental
86 conditions. Starting from empirical results in a limited number of environmental
87 conditions, this modelling framework allows these results to be extrapolated in order to
88 predict the metabolic responses of individuals in other environmental conditions (Reid
89 et al., 2020). Bioenergetic models are based on the fluxes and conservation of energy in
90 physiological processes, in which energy available for somatic growth is estimated as a
91 result of feeding and excretion (Brett and Groves, 1979). The model chosen in this
92 study was the Dynamic Energy Budget (DEB) model (Kooijman, 2010), which is based
93 on the use of energy by an organism for physiological processes such as food

94 assimilation, growth, maintenance and reproduction. This model has been demonstrated
95 to correctly model the lifecycle of a wide range of species, from bacteria to large
96 mammals. The framework provided by the DEB theory allows the quantification of
97 processes of interest for aquaculture (such as growth and feeding efficiency) and of
98 increasing interest for IMTA (such as the bioremediation capacity of extractive species)
99 (Reid et al., 2020, Chary et al., 2020). The associated DEB parameters for more than
100 2000 modelled species to date are available on the online platform Add-my-Pet (AmP)
101 (www.bio.vu.nl/thb/deb/deblab/add_my_pet). Of these species, 7 are polychaetes, with
102 the recent additions of *Arenicola marina* (De Cubber et al., 2019) and *Hediste*
103 *diversicolor* (Lefebvre, 2019). These DEB model parameters for *H. diversicolor* can
104 now be used to predict metabolic processes under different environmental conditions.

105 The aim of this study was to analyze the mitigation potential of deposit-feeding *H.*
106 *diversicolor* in co-cultivation with finfish. The objectives were (1) to validate the DEB
107 model using new datasets obtained through laboratory experiments on growth rates and
108 ammonia excretion, as well as data on oxygen consumption published independently of
109 the calibration procedure, (2) to evaluate the effects of seawater temperatures (5°C to
110 25°C) and assimilation rates (from *ad libitum* to half an *ad libitum* ration) on some life
111 history traits of *H. diversicolor*, and (3) to quantify the bioremediation potential of *H.*
112 *diversicolor* in different aquaculture contexts.

113

114 **2. Material and methods**

115 **2.1. The DEB theory and the lifecycle of *H. diversicolor***

116 A general presentation of the DEB theory and its mathematical formulation is presented
117 in ‘Supplementary material’ (see S1). To perform the DEB simulations for *H.*

118 *diversicolor*, we used the available parameters in the AmP database (Lefebvre, 2019)
119 (Table 1), using an abj-model. Essentially, the DEB theory is based on the assumption
120 that assimilated energy first enters a reserve compartment (E). A fixed fraction (κ) of
121 the energy flux coming from the reserve is then utilized, first for somatic maintenance
122 costs and the remaining part for growth of the structural volume (V). The other fraction
123 (1- κ) is spent on maturation (E_H) in juveniles or on reproduction (E_R) in adults, after
124 having paid the maturity maintenance costs (Figure 1). Acquisition processes (i.e.
125 ingestion and assimilation) are linked to the organism's surface area, while somatic
126 maintenance is proportional to its volume. In contrast to the standard version of the
127 DEB model (std), the abj-model considers a metabolic acceleration between birth and
128 metamorphosis (see S1). Consequently, we scaled maximum surface-specific
129 assimilation ($\{\dot{p}_{Am}\}$) and energy conductance (\dot{v}) to the organism's structural length
130 between birth and metamorphosis, following Kooijman et al. (2011). Finally, as it is a
131 semelparous species, *H. diversicolor* dies after its first reproduction (Olive and
132 Garwood, 1981). Therefore, the maximum structural length L_m was the structural length
133 of the animal that attains first reproduction. In DEB theory, authors refer to this
134 reproductive strategy as 'suicide reproduction' (Kooijman, 2010).

135 The DEB model describes changes in the energy content of four state variables (E, V,
136 E_H and E_R for adults), which cannot be measured directly. The volumetric structural
137 length ($L=V^{1/3}$) can be approximated by the shape-corrected physical (observable)
138 length ($\delta_M L_w$). In this study, the length (cm) of the first three segments (L3: the
139 combined length of the prostomium, peristomium and the first setiger) was used as the
140 physical length, as this is more reliable than the total length in polychaetes. Wet weight
141 (WW) was calculated as the sum of the wet mass of the structure and the wet mass of
142 the reserve (see S1). The wet mass of the reproductive buffer was not included in the

143 WW calculation because it was considered negligible most of the time (GSI<3%, see
144 below).

145

146 **2.2. *H. diversicolor* growth performance in controlled environments**

147 **2.2.1. Sampling.** *H. diversicolor* individuals were collected in the wild in Arnel
148 Lagoon, on the French Mediterranean coast. The experiments were conducted in the
149 Ifremer marine aquaculture experimental station (Palavas-les-Flots, France). For the
150 oxygen and excretion experiments, individuals were acclimatized for 10 days (see
151 details below). For the growth experiment, *in vitro* reproduction was carried out in
152 October 2016 in order to begin with individuals of the same age. During the early larvae
153 stage (from 0 to 22 days), the polychaete offspring were fed with microalgae (*Chlorella*
154 *sp.*), which were cultured at the experimental station and can be ingested (this was
155 confirmed by microscopic observation of the gut content). Before the beginning of the
156 growth experiment, juveniles (from 22 to 113 days), were fed with fish faeces and
157 raised at temperatures ranging between 15°C and 18°C. This food was chosen because
158 fish farm waste is mainly composed of fish faeces and a varying proportion of uneaten
159 fish feed (Galasso et al., 2017).

160

161 **2.2.2 Growth rates.** The growth experiment was conducted on individuals when they
162 reached 113 days of age; the experiment lasted 98 days (February–April 2017). Two
163 types of feed were tested: faeces from farmed European seabass *Dicentrarchus labrax*
164 (Fish faeces) and commercial fish feed (Fish feed). The collection and preparation of
165 these are detailed in Galasso et al. (2017). The fish faeces were composed of 72%
166 organic matter (OM) (including 3% total organic nitrogen [TON] and 7% total lipids
167 [TL]), and 28% ash. The commercial fish feed was composed of 87% OM (including

168 7% TON and 12% TL) and 12% ash. Polychaetes were fed *ad libitum* (based on the
169 observation of leftover food in the tank) from 48 mg.feed.ind⁻¹.d⁻¹ to 85 mg.ind⁻¹.d⁻¹
170 (from the beginning to the end of the experiment). The 113 ± 1 day-old individuals
171 (days post-fertilization) at the start of the growth experiment measured on average 1.16
172 ± 0.24 mm L3. Each treatment was performed in small tanks (4 L) in triplicate (6 tanks;
173 18 polychaetes per tank; total of 108 worms). The water temperature was maintained at
174 17 ± 1°C and at a salinity of 18 ± 1 psu (temperature and salinity conditions favourable
175 to *Hediste* growth) (Olivier et al., 1996; Batista et al., 2003). The worms were reared
176 without sediment, but plastic tubes (Ø = 4 mm; several lengths) were added to provide
177 refuge to reduce stress (adapted from Nesto et al., 2018). The tanks were continuously
178 aerated to maintain oxygen concentration close to saturation for the given temperature
179 (Galasso et al., 2018). Individual wet weight was measured on days 177 and 211, and
180 individual L3 length on days 113, 144, 177 and 211. The worms were weighed
181 individually after a fasting period of 24 h to empty their digestive tract. They were then
182 carefully taken from the water using a dip net, cleaned with seawater and dried on paper
183 towels before being weighed on an analytical balance with a precision of 0.001 g.
184 Specific growth rate was calculated as $SGR = \frac{\log WW_f - \log WW_i}{t_f} \times 100$, where WW_i and
185 WW_f is the wet weight (g) at the beginning and the end of the experiment respectively,
186 and t is the experiment duration (d) (Hopkins, 1992). A Two-way Anova was performed
187 to test the effect of food type (fixed factor, n= 2, Fish feed and Fish faeces) and tank
188 (random factor, n=3) on WW and L3 at each biometry data. In total, 54 individuals were
189 measured per food type.

190 **2.2.3 Oxygen consumption.** The oxygen consumption rates of the ragworms were
191 recorded as a proxy of the minimal metabolic rate (the standard metabolic rate) at four
192 temperatures (11°C, 17°C, 22°C and 27°C). The oxygen consumption could be

193 considered a proxy of the minimal metabolic rate as it was measured on individuals that
194 had fasted for 24 h in the dark. A detailed description of the experiments and results are
195 presented in Galasso et al. (2018). The individuals ranged from 0.02 to 0.57 g WW, and
196 1.40 to 3.64 mm L3. The polychaetes were acclimatized for 10 days and fed *ad libitum*
197 with seabass *Dicentrarchus labrax* faeces, then acclimatized for 7 days at the
198 experimental temperature conditions. The incubation times were chosen to prevent
199 oxygen saturation from dropping below 80%. Consequently, incubation times varied
200 from 4 h (for the aquariums at 22°C and 27°C) to 5 h (for those at 11°C and 17°C). The
201 results were expressed in $\mu\text{mol/h}$.

202

203 **2.2.4 Ammonia excretion.** An ammonia excretion experiment was performed
204 simultaneously with oxygen consumption measurements. Water samples (50 mL) were
205 taken at the beginning of the experiment (t_0) (filtered seawater was used to fill the
206 individual chambers) and at the end of incubation (t_f), and immediately frozen at -20°C
207 for further ammonium analyses (N-NH_4). The ammonium concentrations were
208 measured using Seal AA3 analytical autoanalyser standard methods (Aminot and
209 K  rouel, 2007) with fluorometric detection (from JASCO, FP-2020plus, France).
210 Ammonia excretion rates were determined following the equation used by Galasso et al.
211 (2018) for oxygen. N-NH_4 was transformed to N-NH_3 using the conversion factor 1.22
212 (based on molar mass).

213 **2.3. Comparison between predicted and observed data**

214 Simulations were then carried out to compare the output of the model to data from
215 laboratory experiments on growth performance, oxygen consumption (J_O) and ammonia

216 excretion (\dot{J}_N). In DEB theory, \dot{J}_O and \dot{J}_N are weighted sums of three basic fluxes:
217 assimilation (\dot{p}_A), dissipation (\dot{p}_D) and growth (\dot{p}_G) (see S1 for details and equations).
218 First, optimizations of scaled functional response (f) were performed to evaluate the
219 assimilation rate of the polychaetes. This was performed using the `cma_es` function
220 from the `cmaes` package in R (Trautman et al., 2011) run to minimize the mean relative
221 error (MRE) between predicted and observed data. First an f value was obtained for the
222 period prior to the growth experiment (until 113 days of age), and then an f value was
223 fitted for each feeding condition (fish faeces or fish feed) in the growth experiment. The
224 last L3 length was not used in the fitting process because of high size-specific mortality
225 related to reproduction. As individuals become green at maturity (Dales, 1950), we used
226 this criteria to remove these individuals from the group and from the dataset. Water
227 temperatures during the different experiments were included in the model.

228 Second, since the oxygen consumption and ammonia excretion experiment was
229 performed using individuals fed on faeces, the f fitted using the growth experiment on
230 individuals fed faeces was used for simulating these variables. In addition, as the
231 polychaetes used in the respiration and excretion experiment were collected in the wild,
232 the age and life histories of these individuals were unknown. The scaling with the length
233 and weight was therefore obtained using the DEB model run for individuals with
234 identical life histories (but different ages). Therefore, all the observed differences in
235 lengths within this experiment were linked to differences in age. Finally, since the
236 experiment was performed on polychaetes that had been starved for 24 h, we assumed
237 that the oxygen consumption and ammonia excretion associated to energy assimilation
238 was null ($\dot{p}_A = 0$).

239 **2.4. IMTA scenarios: temperature and assimilation rates**

240 **2.4.1 Effects of temperature and assimilation rate variations.** We evaluated the
241 effects of two key factors that may affect growth: temperature and assimilation rates. As
242 temperature is the main factor in metabolism changes, especially in ectotherms (Wieser,
243 1973), the effect of a large range of temperatures from 5°C to 25°C (in 5°C increments),
244 with fixed optimal feeding conditions (scaled functional response, $f=1$), was tested. This
245 range was selected based on temperature variations observed in *H. diversicolor* habitats
246 (Scaps, 2002) and temperatures that are recorded in European aquaculture production
247 from Norway to Mediterranean Sea (ex. Brigolin et al. 2014; Wang et al. 2020).
248 Assimilation rates were also tested, with f ranging from 0.5 to 1 (half ration of *ad*
249 *libitum* to full *ad libitum*) (in 0.1 increments), at a constant 20°C temperature.

250 The gonadosomatic index (GSI) is the ratio between gonad mass and total body mass.
251 Using DEB theory, GSI is estimated as the ratio between the reproduction buffer wet
252 mass and the wet weight of the animal (see S1). The GSI could therefore be estimated
253 for each age in the growth experiment. In parallel, survival was recorded during the
254 growth experiment. It was assumed to be mostly related to the spawning event (and the
255 associated death) of the animals. We posited that spawning was triggered above a
256 certain GSI threshold. The survival curve was fitted over time using a sigmoid function
257 with the `nls` function in R (3.6.2) and Rstudio (1.2.5033). This enabled us to create a
258 link between the estimated GSI and survival. The curve was fitted with a polynomial
259 curve (of degree 5) using the `poly` function in R in order to obtain links between
260 survival and any GSI. Only the results from the growth experiment using faeces were
261 used for these estimations, since faeces are intended to be the most important food
262 source in a well-designed IMTA system. A GSI of 3% was chosen for the
263 bioremediation simulations since survival was high until this threshold (>90%).

264

265 **2.4.2 Bioremediation capacity.** To estimate the bioremediation capacity of polychaete
266 to consume fish solid wastes, total assimilated energy was estimated over a ragworm
267 production cycle (from birth to harvest) in several scenarios (at 20°C with $f=0.5$ or $f=1$,
268 and at 5°C and 25°C with $f=1$). In aquaculture, a good compromise between reaching
269 commercial weight and survival rates has to be found. For each scenario, simulations
270 were either stopped when the GSI reached 3%, or when individual reached 0.5 g WW
271 (minimum polychaete market size, Nesto et al. 2012). Total assimilated energy (J) was
272 then transformed into grams of dry weight (g DW) of faeces considering that the energy
273 content of one g (DW) of fish faeces was 10.4 kJ. We based our estimation on the
274 average composition of seabass faeces: proteins (14%), lipids (4.6%), carbohydrates
275 (12.8%), fibre (40.6%), and ash (28%) (Galasso et al., 2017), and the associated
276 respective energy contents of 23.6 kJ.g⁻¹, 36.2 kJ.g⁻¹, 17.2 kJ.g⁻¹, 8 kJ.g⁻¹ and 0 kJ.g⁻¹
277 (Brigolin et al., 2014; Chary et al., 2020). Based on information provided in another
278 study (Scaps, 2002), we considered a population density of 3700 ind.m⁻² and estimated
279 the bioremediation capacity of a ragworm farm per m² for a year-round production,
280 considering the life expectancy of the ragworms and the control of *H. diversicolor*
281 reproduction (Wang et al., 2020).

282 **3. Results and discussion**

283 The results from our simulations obtained for *H. diversicolor* using DEB theory
284 provided a good fit with new empirical data on growth, oxygen consumption and
285 excretion in aquaculture conditions. This new empirical data set was not used for the
286 optimization of the parameters available online (Lefebvre, 2019), and therefore we
287 applied it in order to independently validate the parameter set.

288 **3.1 Growth rates and food quality.** The effect of the two food types, Fish faeces and
289 Fish feed, on the growth rates of *Hediste diversicolor* are presented in Table 2. After 98
290 days of the experiment, polychaetes fed with Fish faeces had a slightly (NS) higher final
291 weight (0.41 ± 0.17 g) and length ($L3 = 0.30 \pm 0.05$ cm) than those fed with Fish feed
292 ($WW = 0.36 \pm 0.15$ g and $L3 = 0.28 \pm 0.06$ cm). Significant difference between treatment
293 was only observed on day 177 (two-way Anova test, see Table 2). Individual growth
294 rates (from day 113 to 177) were 0.03 mm $L3.d^{-1}$ and 5 mg $WW.d^{-1}$ (3.8% SGR) for
295 faeces, and 0.02 mm $L3.d^{-1}$ and 4.2 mg $WW.d^{-1}$ (3.5% SGR) for feed. We used the DEB
296 model as an explanatory tool to estimate scaled functional response (f) levels in our
297 growth experiment. f were estimated at 0.6 and 0.5, for Fish faeces and Fish feed
298 respectively, resulting in slightly higher growth rates for *H. diversicolor* fed with Fish
299 faeces. The DEB simulation fit well with observed length data in the growth experiment
300 (Figure 2), with an MRE of 0.11. In results obtained in other studies, a high variation in
301 growth rates has been observed in relation to food quality. For example, in similar
302 conditions of temperature and salinity (25 psu, 18°C) and for comparable initial weights
303 (50 mg WW), lower growth rates (2.1 mg $WW.d^{-1}$, 1.8% SGR) were measured for *H.*
304 *diversicolor* fed with macroalgae (Olivier et al., 1996). Meziane and Retiere (2002)
305 obtained even lower growth rates (0.5 to 2.8 mg $WW.d^{-1}$, 0.3% to 1.9% SGR) for
306 ragworms fed with halophyte detritus in similar environmental conditions (15 psu,
307 21°C). However, Fidalgo e Costa et al. (2000) measured growth rates of 14 mg $WW.d^{-1}$
308 (5.5% SGR) feeding *H. diversicolor* with a post-larval shrimp diet (15 psu and 20°C).
309 High growth rates (6% to 12% d^{-1} SGR) were also recorded in Nesto et al. (2012), who
310 tested three different sources of food, including Larviva-Biomar® and a seaweed
311 (*Sargassum muticum*, a low-protein food) in *H. diversicolor* cultures. In fact, this last
312 study was used in the parameter estimation procedure for *H. diversicolor* (Lefebvre,

313 2019, Add-my-Pet), considering a maximal functional response for the best food source
314 ($f=1$). Wang et al. (2019) observed that *H. diversicolor* reared on fish feed (0.025 d⁻¹
315 SGR) grew significantly faster than worms grown on the other diets, including smolt
316 waste (0.012 d⁻¹ SGR). The difference between their growth rates and the rates
317 measured in our study may originate from varying food quality and other different
318 experimental conditions, i.e. presence/absence of sediment. Indeed, in our experiment,
319 food was provided *ad libitum*, suggesting that $f=1$. The fitted f values of 0.5 and 0.6
320 obtained in our study probably result from a lower digestibility of fish waste compared
321 to other food sources (see Lefebvre et al., 2000). Further experiments could be
322 performed to investigate these hypotheses. Nevertheless, our results showed that despite
323 differences in food quality, growth rates were in the range of other studies. More
324 importantly, although fish waste does not lead to the best SGR compared to other
325 studies, our results indicate that it is a suitable food type for the development, growth
326 and reproduction of *H. diversicolor* in the context of IMTA.

327

328 **3.2 Suicide reproduction and GSI.** It is important to anticipate reproduction,
329 especially when it is associated to death, as is the case for semelparous species. In
330 ragworm aquaculture, harvesting would have to be performed just before reproduction
331 when worms have reached minimum market size (0.5 g WW, Nesto et al., 2012). In our
332 study, observations of the first mortalities attributed to suicide reproduction were made
333 on day 144 (mean survival of 94%). On day 211, mortality reached 43% for individuals
334 fed fish faeces and 52% for individuals fed fish feed. Using DEB simulation, we were
335 able to attribute a GSI to these individuals (Figure 3). We used a GSI of 3% as a
336 threshold for harvesting the individuals during the bioremediation simulations. Indeed,
337 under a GSI of 3%, a survival rate above 90% was estimated (Figure 3). This threshold

338 was estimated from our growth experiment only. Further studies in which GSI is
339 measured on live animals are therefore needed to confirm this threshold. Environmental
340 factors may greatly influence reproduction, including temperature and photoperiod
341 variations (Scaps, 2002; Nesto et al., 2018). In a natural environment, Olive and
342 Garwood (1981) observed the first appearance of developed oocytes in *H. diversicolor*
343 coelom after 18 months. In our study, polychaetes started to reproduce after 5 months,
344 which may indicate that aquaculture conditions with a stable temperature and stable
345 feed input were more favourable to ragworms than natural conditions. Maturation
346 around 4 months under control environment has been observed previously (Nesto et al.,
347 2012). The DEB framework allows simulations to be performed in an environment in
348 which food and temperature vary over time, and therefore estimations of *in situ* age at
349 death (i.e. reproduction) could be performed in the wild as long as temperatures and
350 food conditions are available.

351

352 **3.3 Oxygen consumption and ammonia excretion rates.** The results showed that
353 oxygen consumption (metabolic rate) and ammonia excretion rates increased with body
354 size (WW and L3) and temperature (Figures 4 and 5). The DEB outputs for oxygen
355 consumption and ammonia excretion at different temperatures correctly fit observed
356 data despite the wide variability in oxygen consumption, ranging from 0.09 to 2.35
357 $\mu\text{mol}\cdot\text{h}^{-1}$ (Figure 4) (Galasso et al., 2018), and ammonia excretion, ranging from $4\cdot 10^{-6}$
358 to $0.58 \mu\text{mol}\cdot\text{h}^{-1}$ (Figure 5). The fit between the oxygen consumption data and the
359 predictions was better than for the ammonia excretion data, with respective MREs of
360 0.51 and 0.80. It appeared that the ammonia results were underestimated by the model.
361 The ammonia results were more scattered than the oxygen consumption rate results. The
362 incubation times was short to keep a good oxygen saturation and concentrations were

363 close to the detection limit. A longer incubation period and no previous starvation may
364 have provided less variable data. In marine species, an increase in ammonia excretion
365 with increased temperature is well known, including for invertebrates (Chen and Lai,
366 1993). In contrast to fish, very little is known regarding the ammonia excretion
367 mechanism and the participating excretory organs in marine invertebrates, especially in
368 polychaetes (Thiel et al., 2017). Thus, our study provides valuable data on this topic,
369 which will need further quantitative data in order to properly characterize nutrient fluxes
370 in IMTAs.

371

372 **3.4 Bioremediation potential.** We found that growth rates increased with increasing
373 temperatures (Figure 6) and scaled functional response (f , Figure 7). For the
374 bioremediation estimation, simulations were stopped when GSI reached 3% or 0.5 g
375 WW, considered as the minimum market size. The results from selected scenarios are
376 shown in Table 3. At 20°C, an increased assimilation rate (higher f) reduced the time to
377 reach the GSI threshold (99 days with $f=0.5$ vs 79 days with $f=1$). At this stage,
378 ragworms weighed only 0.2 g at $f=0.5$ compared to 0.6 g when $f=1$. At the maximum
379 assimilation rate ($f=1$), increased temperature (5°C vs 25°C) decreased the time to reach
380 a GSI of 3% (163 days at 5°C vs 64 days at 25°C), but had no effect on the final wet
381 weight (0.6 g). Similar observations were made when simulations were stopped at a wet
382 weight of 0.5 g. It should be noted that at 20°C with $f=0.5$, the minimum market size of
383 0.5 g was reached in 128 days, but with a GSI of 3.9%. In a bioremediation perspective,
384 the potential of *H. diversicolor* was estimated based on cumulated assimilation rates
385 (\dot{p}_A). Assuming an energy content of 10.4 kJ.g⁻¹ DW of seabass faeces, and based on the
386 high density of *H. diversicolor* (3700 ind. m⁻²) reported in nature (Scaps, 2002), we
387 estimated a bioremediation capacity ranging from 0.23 to 0.87 g faeces DW ind⁻¹ year⁻¹,

388 eq of 755 to 2887 g faeces DW m⁻² year⁻¹ (Table 3). This could represent 75-289 kg for
389 a 100 m² ragworm farm, equivalent to a 2-9 % reduction in the waste produced by a
390 20T seabass farm (160 kg of DW faeces per ton of seabass production, based on
391 assimilation coefficients in Brigolin et al., 2014). This study therefore confirms the
392 potential of *H. diversicolor* in IMTA systems, in particular associated with fish farms,
393 as has been shown in previous studies (Batista et al., 2003; Bischoff et al., 2009; Cubillo
394 et al., 2016 and Marques et al., 2017). Comparisons of bioremediation capacity to other
395 studies are, however, difficult as most of previous studies are site specific or based on
396 specific scenario. The quantity of faeces produced by a marine fish farms depends on
397 numerous factors (species, conversion ratio, temperature, farm management, etc) and
398 can vary from 160 kg of DW faeces per ton of seabass production (Brigolin et al., 2014)
399 to 224 Kg of DW faeces per ton of salmon production (see review by van Rijn, 2013).
400 Wang et al. (2019) estimated that 1 Kg of fish released 250 g of faeces and 30 g of
401 uneaten feed and could produce 800 g of *H. diversicolor*. Considering the feed
402 conversion ratio (g dry faeces used/g polychaete biomass produced) of 3.55 given by
403 the authors, we could estimate a bioremediation capacity of 23 g of fish faeces, eq 9.2 %
404 of faeces reduction (ragworm density was not provided in this study). Chary et al.
405 (2020) compared studies using mathematical models to examine uptake of solid organic
406 matter or nutrients in IMTA systems by other detritivores. Conclusions were quite
407 contrasted (Chary et al., 2020). Cubillo et al. (2016) and Ren et al. (2012) predicted that
408 bottom culture of sea cucumbers could remove more than 70% of the benthic particulate
409 organic carbon (C) from Atlantic salmon (*Salmo salar*) farm units. These two studies
410 did not consider rearing constraints (limit of density) for the extractive species.
411 Including such considerations in models can help predict more realistic production
412 design and bioremediation potentials from extractive species. When considering current

413 density rearing practices, Watanabe et al. (2015) calculated that 4.3% of total particulate
414 nitrogen from milkfish (*Chanos chanos*) culture could be removed by seacumber
415 detritivore species. In the present study, the bioremediation potential was expressed per
416 individual and per m⁻², and for a large range of temperature, to allow future
417 comparisons. The DEB model allows simulations to be performed that may be useful to
418 predict life history traits in different environmental conditions, as well as to anticipate
419 harvest before reproduction.

420 **Conclusion.** Our results suggest that fish waste could constitute the exclusive source of
421 food for the polychaete *Hediste diversicolor*. We were able to obtain these results using
422 a DEB model that accurately predicted the species' metabolic processes. Further studies
423 could build on these results by including certain environmental factors, such as water
424 salinity, photoperiod, as well as other water temperature variations that may trigger
425 reproduction. These findings suggest that DEB modelling is a promising tool for IMTA
426 development. The method could help fish producers manage the use of *H. diversicolor*
427 to complement their primary production and could also assist environmental policy by
428 utilizing the bioremediation potential of *H. diversicolor* when associated to fish
429 production.

430 **Acknowledgements**

431 The authors would like to thank Luca Florean, Osvaldo Makowiecky and Alexandre
432 Dousset for their valuable help reviewing life history traits and in the laboratory,
433 Thibault Geoffroy and Sébastien Triplet for their participation in the experimental work,
434 and Marion Richard for her great help planning and conducting the oxygen
435 consumption experiments. We thank two anonymous reviewers for their constructive
436 comments, which helped us to improve the manuscript. We also thank Elise Bradbury
437 for careful revision of the English. The study was carried out within the framework of

438 the ERA-Net COFASP (Strengthening Cooperation in European Research on
439 Sustainable Exploitation of Marine Resources in Seafood Chains) project (IMTA-Effect
440 project) with funding from the French National Research Agency (ANR-15-COFA-
441 0001-06). It was also supported by the Brazilian government's 'Science Without
442 Borders' programme (CAPES PhD scholarship n°13.773-13-5 awarded to HG) and the
443 European Maritime and Fisheries Fund (EPURVAL2 project) (postdoctoral grant
444 awarded to BS).

445 **4. References**

- 446
447 Abreu, M.H., Pereira, R., Yarish, C., Buschmann, A.H., Sousa-Pinto, I., 2011. IMTA
448 with *Gracilaria vermiculophylla*: Productivity and nutrient removal performance
449 of the seaweed in a land-based pilot scale system. *Aquaculture* 312, 77–87.
450 doi:10.1016/j.aquaculture.2010.12.036
- 451 Aminot, A., K erouel, R., 2007. Dosage automatique des nutriments dans les eaux
452 marines.
- 453 Batista, F.M., Fidalgo e Costa, P., Ramos, A., Passos, A.M., Pous o Ferreira, P.,
454 Cancela da Fonseca, L., 2003. Production of the ragworm *Nereis diversicolor*
455 (O. F. M uller, 1776), fed with a diet for gilthead seabream *Sparus auratus* L.,
456 1758: survival, growth, feed utilization and oogenesis. *Inst. Espa ol Oceanogr.*
457 19, 447–451.
- 458 Bischoff, A.A., Fink, P., Waller, U., 2009. The fatty acid composition of *Nereis*
459 *diversicolor* cultured in an integrated recirculated system: Possible implications
460 for aquaculture. *Aquaculture* 296, 271–276.
461 doi:10.1016/j.aquaculture.2009.09.002
- 462 Brett, J.R., Groves, T.D.D., 1979. Physiological Energetics. Vol. VIII- Bioenergetics
463 and Growth, in: Hoar W.S., Randall, D.J., Brett, J.R. (Eds.), *Fish Physiology*.
464 Academic Press, London, pp. 288–344.
- 465 Brigolin, D., Pastres, R., Tomassetti, P., Porrello, S., 2010. Modelling the biomass yield
466 and the impact of seabream mariculture in the Adriatic and Tyrrhenian Seas
467 (Italy). *Aquac. Int.* 18, 149–163. <https://doi.org/10.1007/s10499-008-9232-4>
- 468 Brigolin, D., Meccia, V. L., Venier, C., Tomassetti, P., Porrello, S., Pastres, R., 2014.
469 Modelling biogeochemical fluxes across a Mediterranean fish cage farm.
470 *Aquaculture Environment Interactions* 5(1): 71-88.
- 471 Cammen, L.M., 1980. The significance of microbial carbon in the nutrition of the
472 deposit feeding Polychaete *Nereis succinea*. *Mar. Biol.* 61, 9–20.
- 473 Chary, K., Aubin, J., Sadoul, B., Fiandrino, A., Cov es, D., Callier, M. D., 2020.
474 Integrated multi-trophic aquaculture of red drum (*Sciaenops ocellatus*) and sea
475 cucumber (*Holothuria scabra*): Assessing bioremediation and life-cycle impacts.
476 *Aquaculture*, 516. 734621 (17p.). doi.org/10.1016/j.aquaculture.2019.734621
- 477 Chen, J.-C., Lai, S.-H., 1993. Effects of temperature and salinity on oxygen
478 consumption and ammonia excretion of juvenile *Penaeus japonicus* Bate. *J. Exp.*
479 *Mar. Bio. Ecol.* 165, 161–170589. doi:10.1007/s10499-008-9169-7
- 480 Chopin, T., Cooper, J.A., Reid, G., Cross, S., Moore, C., 2012. Open-water integrated
481 multi-trophic aquaculture: environmental biomitigation and economic
482 diversification of fed aquaculture by extractive aquaculture. *Rev. Aquac.* 4, 209–
483 220. doi:10.1111/j.1753-5131.2012.01074.x
- 484 Cook, E.J., Kelly, M.S., 2007. Enhanced production of the sea urchin *Paracentrotus*
485 *lividus* in integrated open-water cultivation with Atlantic salmon *Salmo salar*.
486 *Aquaculture* 273, 573–585. doi:10.1016/j.aquaculture.2007.10.038
- 487 Cubillo, A.M., Ferreira, J.G., Robinson, S.M.C.C., Pearce, C.M., Corner, R.A.,
488 Johansen, J., 2016. Role of deposit feeders in integrated multi-trophic
489 aquaculture - A model analysis. *Aquaculture* 453, 54–66.
490 doi:10.1016/j.aquaculture.2015.11.031
- 491 De Cubber, L., Lefebvre, S., Lancelot, T., Denis, L., & Gaudron, S. M., 2019. Annelid
492 polychaetes experience metabolic acceleration as other Lophotrochozoans:
493 Inferences on the life cycle of *Arenicola marina* with a Dynamic Energy Budget
494 model. *Ecological Modelling*, 411. doi.org/10.1016/j.ecolmodel.2019.108773

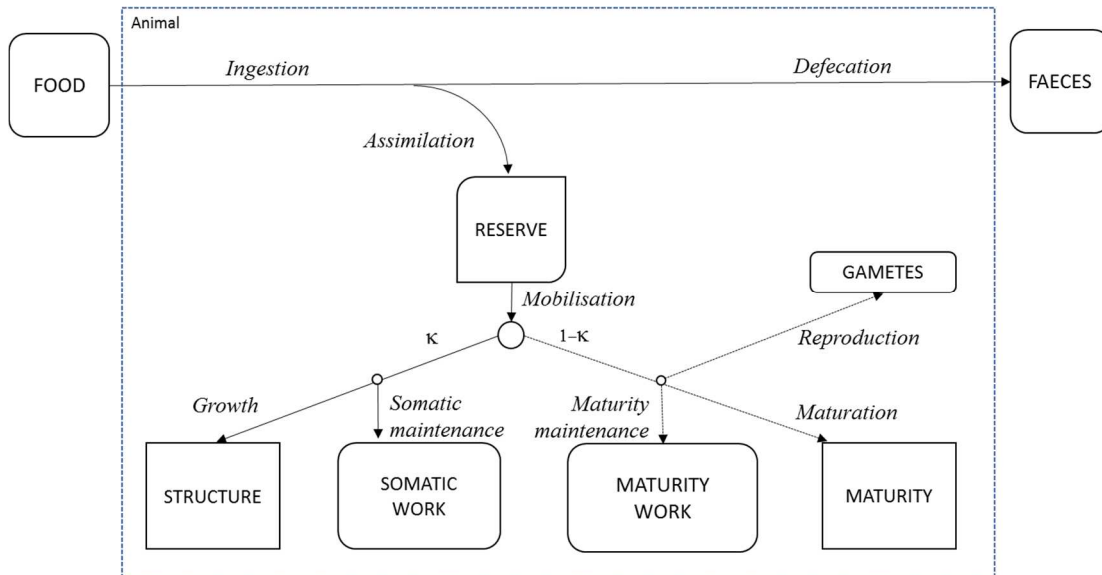
- 495 Erler, D. V, Pollard, P.C., Burke, M., Knibb, W., 2000. Biological remediation of aqua-
496 culture waste: a combined finfish, artificial substrate treatment system, in:
497 Proceedings of the National Workshop of Wastewater Treatment and Integrated
498 Aquaculture. pp. 93–107.
- 499 Fang, J., Jiang, Z., Jansen, H.M., H U, F., Fang, J., Liu, Y., Gao, Y., Du, M., 2017.
500 Applicability of *Perinereis aibuhitensis* Grube for fish waste removal from fish
501 cages in Sanggou Bay, P. R. China. Ocean. Coast. Sea Res. 16, 294–304.
502 doi:10.1007/s11802-017-3256-1
- 503 Fidalgo e Costa, P., Narciso, L., Fonseca, L.C., 2000. Growth, survival and fatty acid
504 profile of *Nereis diversicolor* (O. F. Müller, 1776) fed on six different diets.
505 Bulletin of Marine Science, 67(1): 337–343.
- 506 Filgueira, R., Guyondet, T., Reid, G.K., Grant, J., Cranford, P.J., 2017. Vertical particle
507 fluxes dominate integrated multi-trophic aquaculture (IMTA) sites: implications
508 for shellfish – finfish synergy 9, 127–143.
- 509 Galasso, H.L., Callier, M. D., Bastianelli, D., Blancheton, J.-P., & Aliaume, C., 2017.
510 The potential of near infrared spectroscopy (NIRS) to measure the chemical
511 composition of aquaculture solid waste. Aquaculture, 476.
512 <https://doi.org/10.1016/j.aquaculture.2017.02.035>
- 513 Galasso, Helena Lopes, Richard, M., Lefebvre, S., Aliaume, C., & Callier, M. D., 2018.
514 Body size and temperature effects on standard metabolic rate for determining
515 metabolic scope for activity of the polychaete *Hediste (Nereis) diversicolor*.
516 PeerJ, 6. <https://doi.org/10.7717/peerj.5675>
- 517 Gillet, P., Mouloud, M., Durou, C., Deutsch, B., 2008. Response of *Nereis diversicolor*
518 population (Polychaeta, Nereididae) to the pollution impact – Authie and Seine
519 estuaries (France). Estuar. Coast. Shelf Sci. 76, 201–210.
520 doi:10.1016/j.ecss.2007.07.004
- 521 Hargrave, B.T. (Ed.), 2005. Environmental Effects of Marine Finfish Aquaculture,
522 Handbook of Environmental Chemistry. Springer-Verlag, Berlin/Heidelberg.
523 <https://doi.org/10.1007/b12227>
- 524 Hedman, J.E., Gunnarsson, J.S., Samuelsson, G., Gilbert, F., 2011. Particle reworking
525 and solute transport by the sediment-living polychaetes *Marenzelleria neglecta*
526 and *Hediste diversicolor*. J. Exp. Mar. Bio. Ecol. 407, 294–301.
527 doi:10.1016/j.jembe.2011.06.026
- 528 Heilskov, A.C.C., Holmer, M., 2001. Effects of benthic fauna on organic matter
529 mineralization in fish-farm sediments: importance of size and abundance. ICES
530 J. Mar. Sci. 58, 427–434. doi:10.1006/jmsc.2000.1026
- 531 Hopkins, K.D., 1992. Reporting Fish Growth: A Review of the Basics. Journal of the
532 World Aquaculture Society. 23, 173-179
- 533 Jansen, H. M., Broch, O. J., Bannister, R., Cranford, P., Handa, A., Husa, V., Jiang, Z.,
534 Strohmeier, T., Strand, O., 2018. Spatio-temporal dynamics in the dissolved
535 nutrient waste plume from Norwegian salmon cage aquaculture. Aquaculture
536 Environment Interactions 10: 385-399.
- 537 Jiang, Z., Wang, G., Fang, J., Mao, Y., Bay, A., 2013. Growth and food sources of
538 Pacific oyster *Crassostrea gigas* integrated culture with Sea bass *Lateolabrax*.
539 Aquac. Int. 21, 45–52. doi:10.1007/s10499-012-9531-7
- 540 Kooijman, S. (2010). Dynamic Energy Budget theory for metabolic organisation.
541 Cambridge Univ. Press, Cambridge
- 542 Kooijman, S.A.L.M, Pecquerie L., Augustine S, Jusup, M., 2011. Scenarios for
543 acceleration in fish development and the role of metamorphosis. Journal of Sea
544 Research. 66, 4, 419–423

- 545 Katz, T., Herut, B., Genin, A., Angel, D.L., 2002. Gray mullets ameliorate organically
546 enriched sediments below a fish farm in the oligotrophic Gulf of Aqaba (Red
547 Sea). *Mar. Ecol. Prog. Ser.* 234, 205–214. doi:10.3354/meps234205
- 548 Kristensen, E., 1983. Ventilation and oxygen uptake by three species of *Nereis*
549 (Annelida: Polychaeta). II. Effects of temperature and salinity changes. *Mar.*
550 *Ecol. Prog. Ser.* 12, 299–306.
- 551 Lefebvre, S., Barille, L., Clerc, M., 2000. Pacific oyster (*Crassostrea gigas*) feeding
552 responses to a fish-farm effluent. *Aquaculture* 187(1-2): 185-198.
- 553 Lefebvre, S., 2019. AmP *Hediste diversicolor*, version 2019/09/28
- 554 MacDonald, C.L.E., Stead, S.M., Slater, M.J., 2013. Consumption and remediation of
555 European Seabass (*Dicentrarchus labrax*) waste by the sea cucumber *Holothuria*
556 *forskali*. *Aquac. Int.* 21, 1279–1290. doi:10.1007/s10499-013-9629-6
- 557 Marques, B., Calado, R., Lillebø, A.I., 2017. New species for the biomitigation of a
558 super-intensive marine fish farm effluent: Combined use of polychaete-assisted
559 sand filters and halophyte aquaponics. *Sci. Total Environ.* 599–600, 1922–1928.
560 doi:10.1016/j.scitotenv.2017.05.121
- 561 Mermillod-Blondin, F., Rosenberg, R., François-Carcaillet, F., Norling, K., Mauclair,
562 L., 2004. Influence of bioturbation by three benthic infaunal species on
563 microbial communities and biogeochemical processes in marine sediment.
564 *Aquat. Microb. Ecol.* 36, 271–284. doi:10.3354/ame036271
- 565 Meziane, T., Retiere, C., 2002. Growth of *Nereis diversicolor* (L.) juveniles fed with
566 detritus of halophytes. *Oceanol. Acta* 25, 119–124.
- 567 Michaud, E., Desrosiers, G., Mermillod-Blondin, F., Bjorn Sundby, Georges Stora,
568 2006. The functional group approach to bioturbation: II. The effects of the
569 *Macoma balthica* community on fluxes of nutrients and dissolved organic
570 carbon across the sediment–water interface. *Journal of Experimental Marine*
571 *Biology and Ecology*, 337, Issue 2, 178-189
- 572 Nelson, E.J., MacDonald, B. a. A., Robinson, S.M.C., 2012. The absorption efficiency
573 of the suspension-feeding sea cucumber, *Cucumaria frondosa*, and its potential
574 as an extractive integrated multi-trophic aquaculture (IMTA) species.
575 *Aquaculture* 370–371, 19–25. doi:10.1016/j.aquaculture.2012.09.029
- 576 Nesto, N., Simonini, R., Prevedelli, D., Da, L., 2018. Evaluation of different procedures
577 for fertilization and larvae production in *Hediste diversicolor* (O. F. Müller,
578 1776) doi:10.1111/are.13589
- 579 Nesto, N., Simonini, R., Prevedelli, D., Ros, L. Da, 2012. Effects of diet and density on
580 growth, survival and gametogenesis of *Hediste diversicolor* (O. F. Müller, 1776)
581 (Nereididae, Polychaeta). *Aquaculture* 362–363, 1–9.
582 doi:10.1016/j.aquaculture.2012.07.025
- 583 Neori, A., Chopin, T., Troell, M., Buschmann, A.H., Kraemer, G.P., Halling, C.,
584 Shpigel, M., Yarish, C., 2004. Integrated aquaculture: rationale, evolution and
585 state of the art emphasizing seaweed biofiltration in modern mariculture.
586 *Aquaculture* 231, 361–391.
587 doi:http://dx.doi.org/10.1016/j.aquaculture.2003.11.015
- 588 Nielsen, A.M., Eriksen, N.T., Iversen, J.J.L., Riisgård, H.U., 1995. Feeding, growth and
589 respiration in the polychaetes *Nereis diversicolor* (facultative filter feeder) and
590 *N. virens* (omnivorous) - a comparative study. *Mar. Ecol. Prog. Ser.* 125, 149–
591 158. doi:10.3354/meps125149
- 592 Olive, P.J.W., Garwood, P.R.G., 1981. Gametogenic cycle and population structure of
593 *Nereis (Hediste) diversicolor* and *Nereis (Nereis) pelagica* from north-east
594 England. *J. Maine Biol. Ass* 61, 193–213.

- 595 Olivier, M., Desrosiers, G., Caron, A., Ret, 1996. Juvenile growth of the polychaete
596 *Nereis virens* feeding on a range of marine vascular and macroalgal plant
597 sources. *Marine* 125, 693–699.
- 598 Orr, L.C., Curtis, D.L., Cross, S.F., Gurney-Smith, H., Shanks, A., Pearce, C.M., 2014.
599 Ingestion rate, absorption efficiency, oxygen consumption, and fecal production
600 in green sea urchins (*Strongylocentrotus droebachiensis*) fed waste from
601 sablefish (*Anoplopoma fimbria*) culture. *Aquaculture* 422–423, 184–192.
602 doi:10.1016/j.aquaculture.2013.11.030
- 603 Ozoh, P.T.E., Jones, N. V, 1990. The effects of salinity and temperature on the toxicity
604 of copper to 1-day and 7-day-old larvae of *Hediste (Nereis) diversicolor* (O. F.
605 Müller). *Ecotoxicol. Environ. Saf.* 19, 24–32. doi:10.1016/0147-6513(90)90075-
606 G
- 607 Paltzat, D.L., Pearce, C.M., Barnes, P. a. A., McKinley, R.S., 2008. Growth and
608 production of California sea cucumbers (*Parastichopus californicus Stimpson*)
609 co-cultured with suspended Pacific oysters (*Crassostrea gigas Thunberg*).
610 *Aquaculture* 275, 124–137. doi:10.1016/j.aquaculture.2007.12.014
- 611 Papaspyrou, S., Thessalou-Legaki, M., Kristensen, E., 2010. The influence of infaunal
612 (*Nereis diversicolor*) abundance on degradation of organic matter in sandy
613 sediments. *J. Exp. Mar. Bio. Ecol.* 393, 148–157.
614 doi:10.1016/j.jembe.2010.07.015
- 615 Porter, C.B., Krost, P., Gordin, H., Angel, D.L., 1996. Preliminary assessment of grey
616 mullet (*Mugil cephalus*) as a forager of organically enriched sediments below
617 marine fish farms. *Isr. J. Aquac. Bamidgeh* 48, 47–55.
- 618 Ren, J. S., Stenton-Dozey, J., Plew, D. R., Fang, J., & Gall, M., 2012. An ecosystem
619 model for optimising production in integrated multitrophic aquaculture systems.
620 *Ecological Modelling*, 246, 34–46. doi.org/10.1016/j.ecolmodel.2012.07.020
- 621 van Rijn, J. (2013). Waste treatment in recirculating aquaculture systems. *Aquacultural*
622 *Engineering* 53: 49-56.
- 623 Reid, G.K., Lefebvre, S., Filgueira, R., Robinson, S.M.C., Broch, O.J., Dumas A.,
624 Chopin, T.B.R., 2020. Performance measures and models for open-water
625 integrated multi-trophic aquaculture. *Reviews in Aquaculture* 12 (1), 47-75
- 626 Riisgård, H.U., 1994. Filter-feeding in the polychaete *Nereis diversicolor*: a review.
627 *Netherlands J. Aquat. Ecol.* 28, 453–458. doi:10.1007/BF02334216
- 628 Scaps, P., 2002. A review of the biology, ecology and potential use of the common
629 ragworm *Hediste diversicolor* (O. F. Müller) (Annelida: Polychaeta).
630 *Hydrobiologia* 470, 203–218. doi:10.1023/A:1015681605656
- 631 Trautmann, H., Mersmann, O., Arnu, D., 2011. cmaes: Covariance Matrix Adapting
632 Evolutionary Strategy. R package version 1.0-11. [https://CRAN.R-](https://CRAN.R-project.org/package=cmaes)
633 [project.org/package=cmaes](https://CRAN.R-project.org/package=cmaes)
- 634 Wang, H. Q., Seekamp, I., Malzahn, A., Hagemann, A., Carvajal, A. K., Slizyte, R.,
635 Standal, I. B., Handa, A., Reitan, K. I., 2019. Growth and nutritional
636 composition of the polychaete *Hediste diversicolor* (OF Muller, 1776) cultivated
637 on waste from land-based salmon smolt aquaculture. *Aquaculture* 502:232–241.
- 638 Wang, H. Q., Hagemann, A., Reitan, K. I., Handa, A., Uhre, M., Malzahn, A. M., 2020.
639 Embryonic and larval development in the semelparous Nereid polychaete
640 *Hediste diversicolor* (OF Muller, 1776) in Norway: Challenges and perspectives.
641 *Aquaculture Research* 00:1–17.
- 642 Watanabe, S., Kodama, M., Orozco, Z.G.A., Sumbing, J.G., Novilla, S.R.M., Lebata-
643 Ramos, M.J.H., 2015. Estimation of energy budget of sea cucumber, *Holothuria*
644 *scabra*, in integrated multi-trophic aquaculture., in: M. R. R. Romana-Eguia, F.

- 645 D. Parado-Esteva, N. D. Salayo, & M. J. H. Lebata-Ramos (Eds.), Resource
646 Enhancement and Sustainable Aquaculture Practices in Southeast Asia:
647 Challenges in Responsible Production of Aquatic Species: Proceedings of the
648 International. Tigbauan, Iloilo, Philippines Aquaculture Department, Southeast
649 Asian Fisheries Development Center, pp. 307–308
- 650 Wieser, W., 1973. Effects of Temperature on Ectothermic Organisms: Ecological
651 Implications and Mechanisms of Compensation, 1st ed. Springer-Verlag, New
652 York Heidelberg Berlin 1973.
653

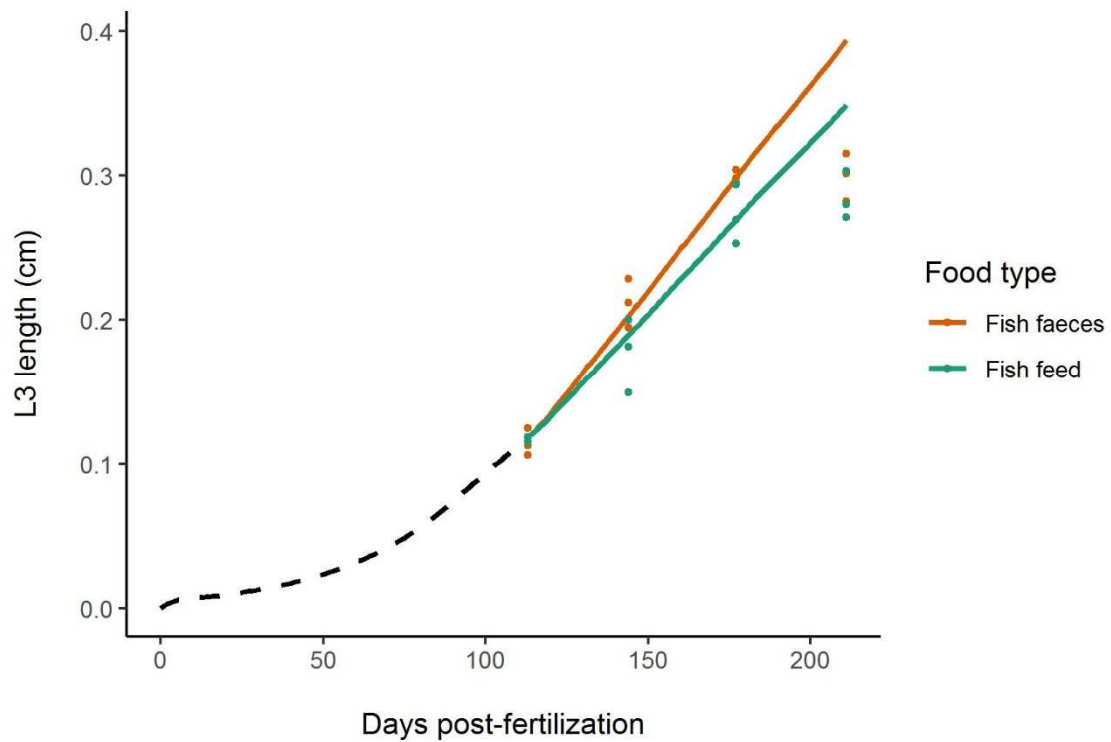
654 Figure 1. DEB representation of allocation rule (κ rule) and energy fluxes in an
 655 organism. Ingested energy is either assimilated or lost by defecation. Then part of the
 656 energy mobilized from the reserve (κ) is allocated for somatic maintenance and growth,
 657 and the remaining energy is spent for maturity and its associated maintenance. Once
 658 sexual maturity is reached, the energy available for maturity is used for the production
 659 of gametes (modified from Kooijman, 2010).
 660



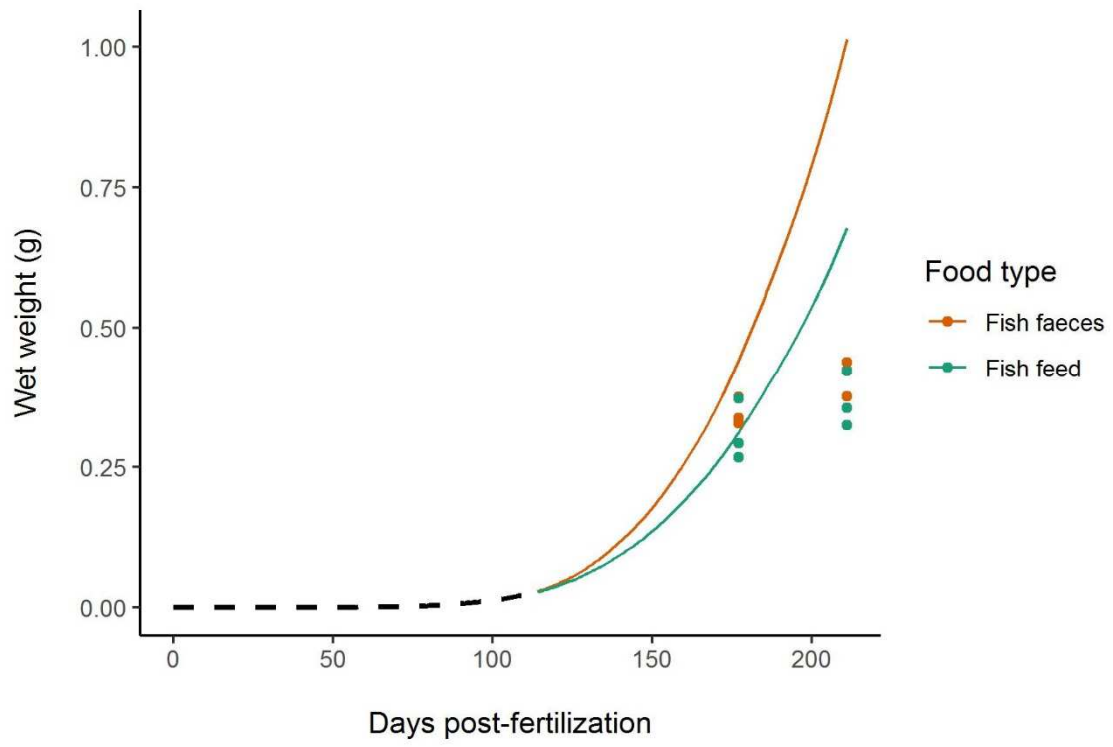
661
 662
 663
 664

665 Figure 2. *Hediste diversicolor*. Comparison of DEB simulation (line) and growth data
 666 (a) L3 length (cm) and (b) wet weight (WW) (g) for polychaetes fed with Fish faeces
 667 and Fish feed. After optimization, $f=0.5$ for Fish feed and $f=0.6$ for Fish faeces. Before
 668 the experiment (dashed line), f was estimated to be 0.4. Individual WW was measured
 669 on days 177 and 211, and individual L3 length on days 113, 144, 177 and 211. The
 670 values obtained during the last biometry (211 days post-fertilization) were not included
 671 in the optimization due to high suicide reproduction. MRE = 0.11 for L3 length values.

672 a)



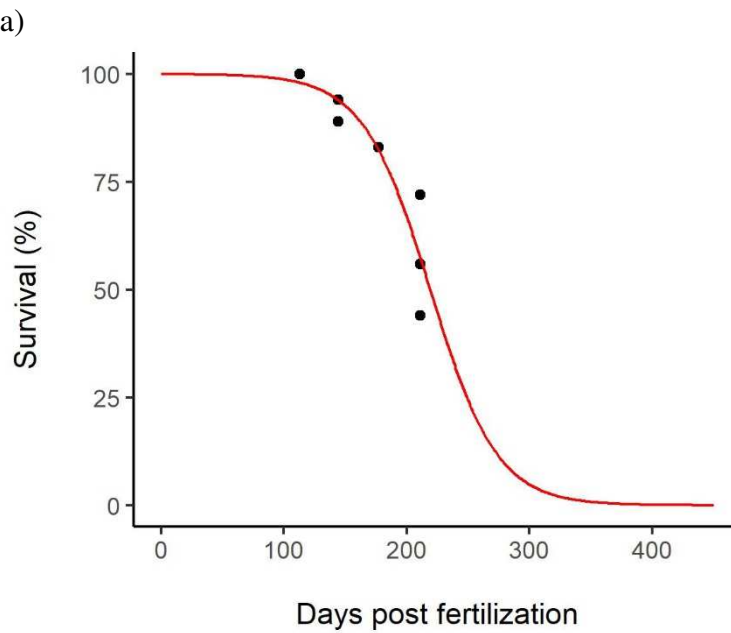
673 b)
 674



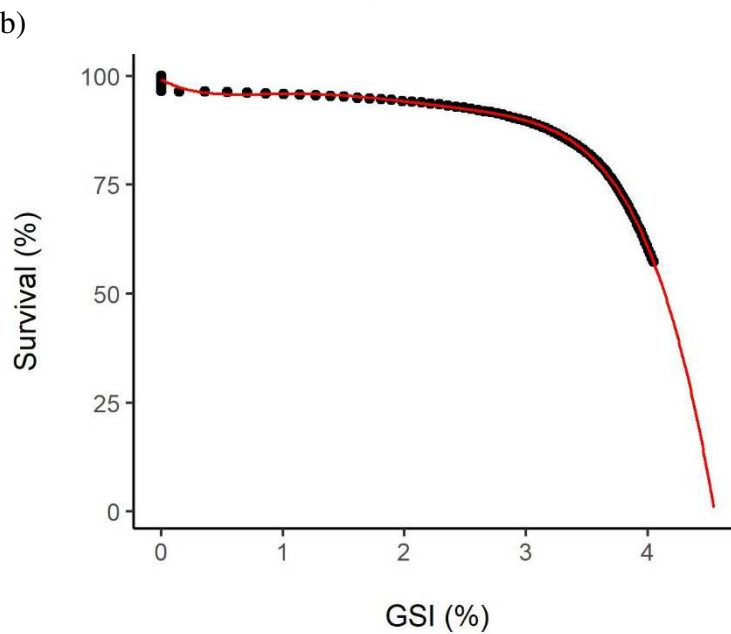
675
676

677 Figure 3. Survival over time and by GSI in polychaetes fed with fish faeces. (a) Survival
 678 over time. The curve was fitted using a sigmoid (red line, $R^2 = 0.87$). (b) Survival by
 679 estimated GSI from the DEB model on ages ranging from 0 to 500 days post-
 680 fertilization. A polynomial function of degree 5 was fitted (red line, $R^2 = 1$).

681
 682



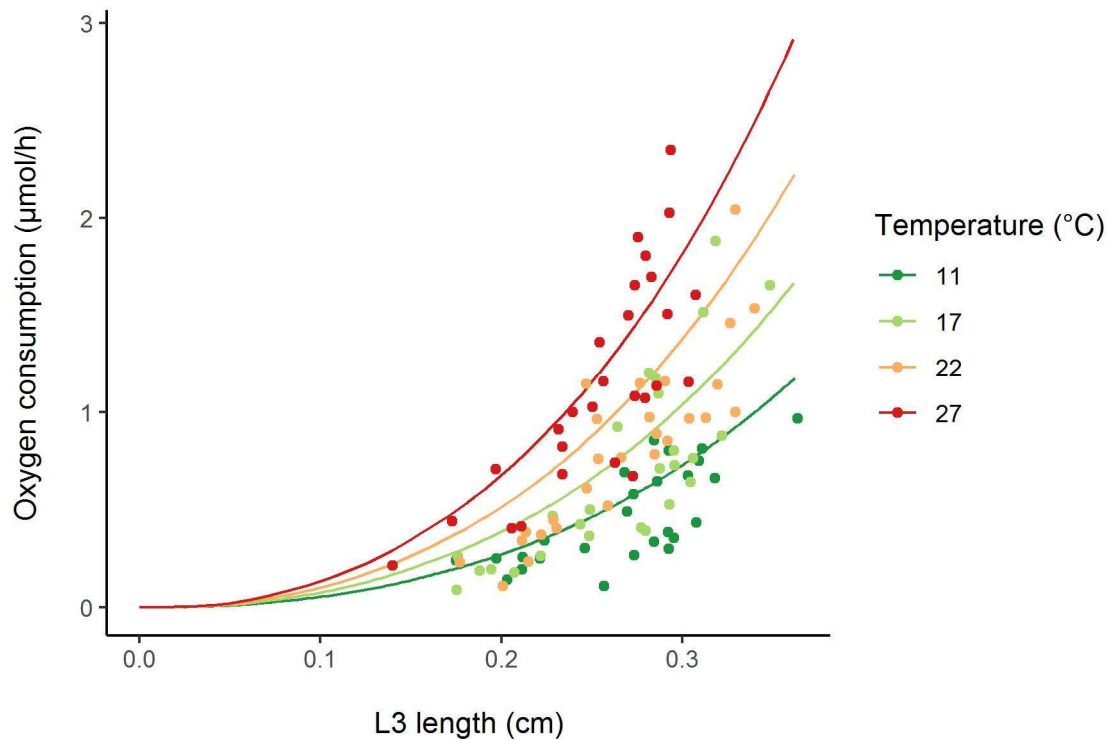
683
 684



685
 686
 687
 688

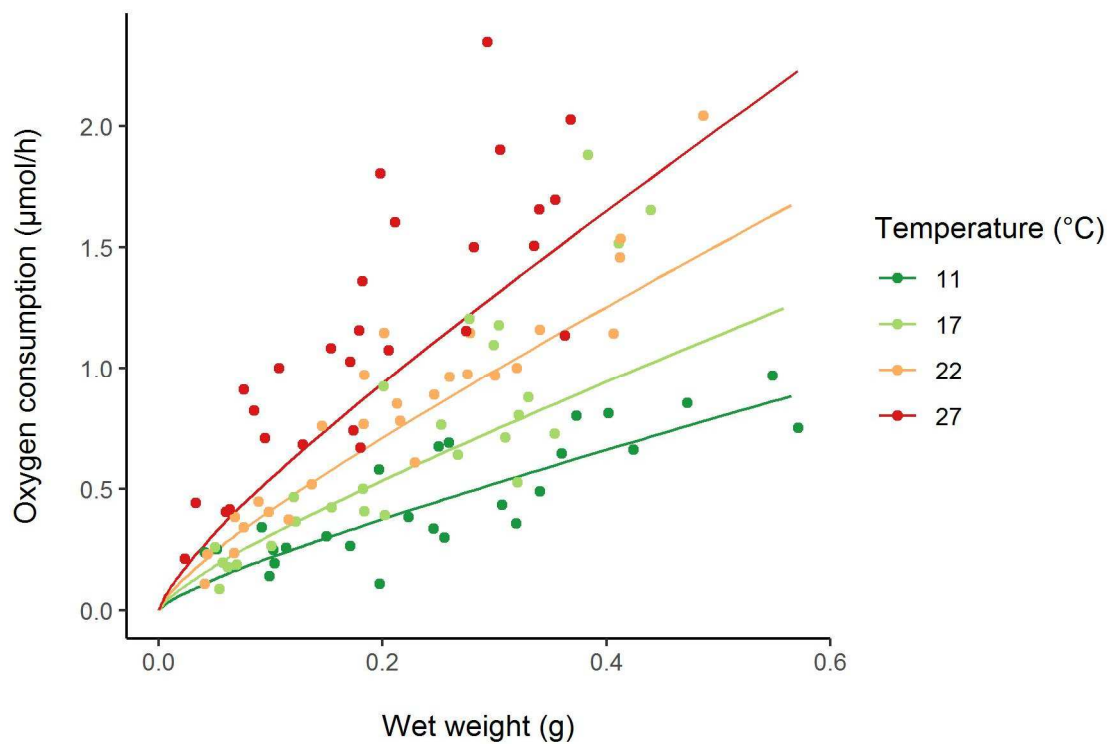
689 Figure 4. *Hediste diversicolor*. Comparison of DEB simulation (line) and oxygen
 690 consumption rates at four temperatures (11°C, 17°C, 22°C and 27°C) expressed over (a)
 691 L3 length (cm) and (b) wet weight (WW) (g) for polychaetes fed with fish faeces (f
 692 =0.6). MRE = 0.51 for L3 length and WW values.

693 a)



694

695 b)

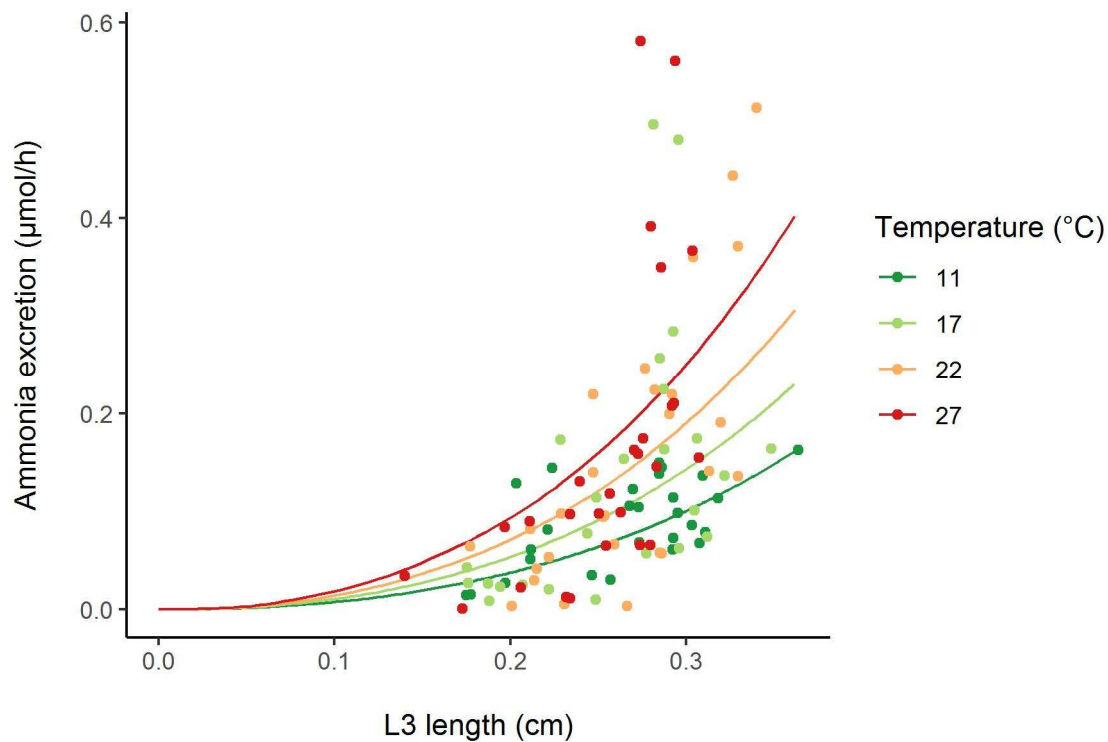


696

697

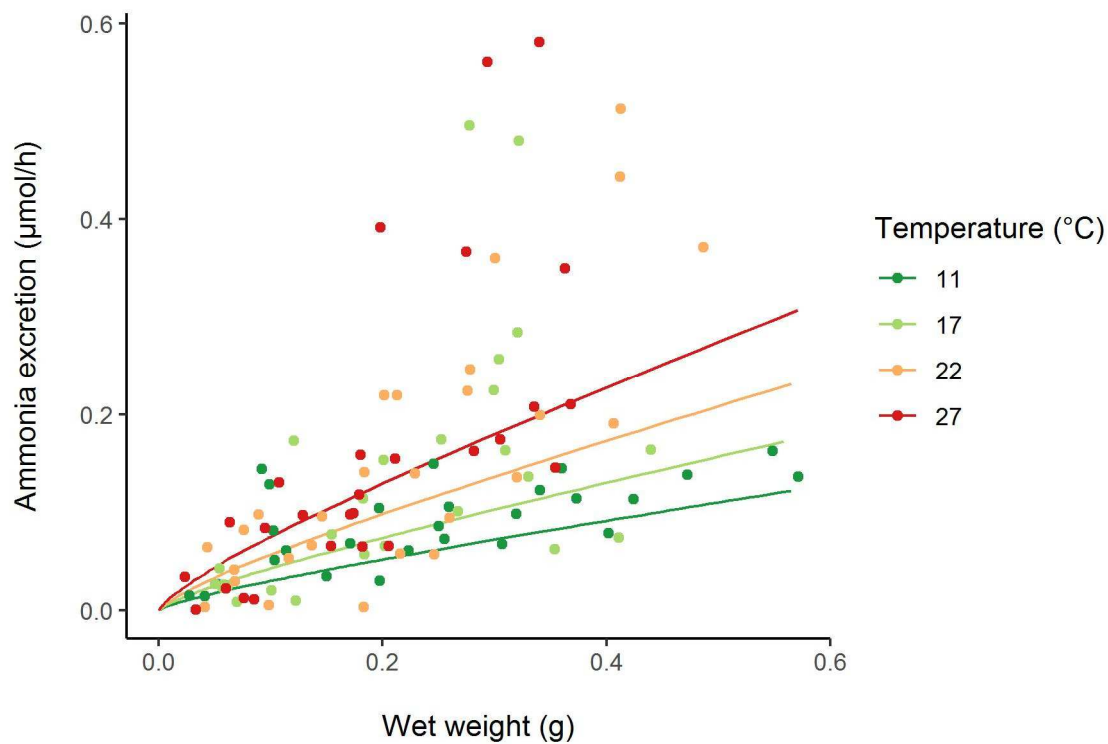
698 Figure 5. *Hediste diversicolor*. Comparison of DEB simulation (line) and ammonia
699 excretion rates at four temperatures (11°C, 17°C, 22°C and 27°C) expressed over (a) L3
700 length (cm) and (b) wet weight (WW) (g) for polychaetes fed with fish faeces ($f=0.6$).
701 MRE = 0.8 for L3 length and WW values.

702 a)



703

704 b)

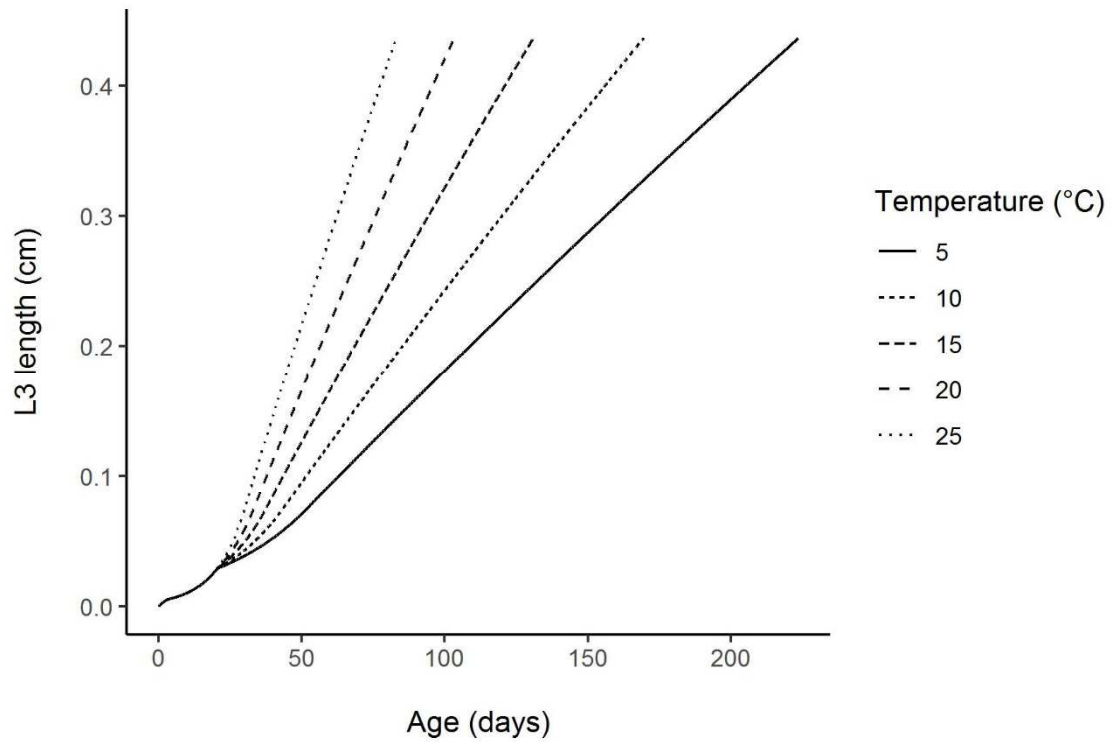


705

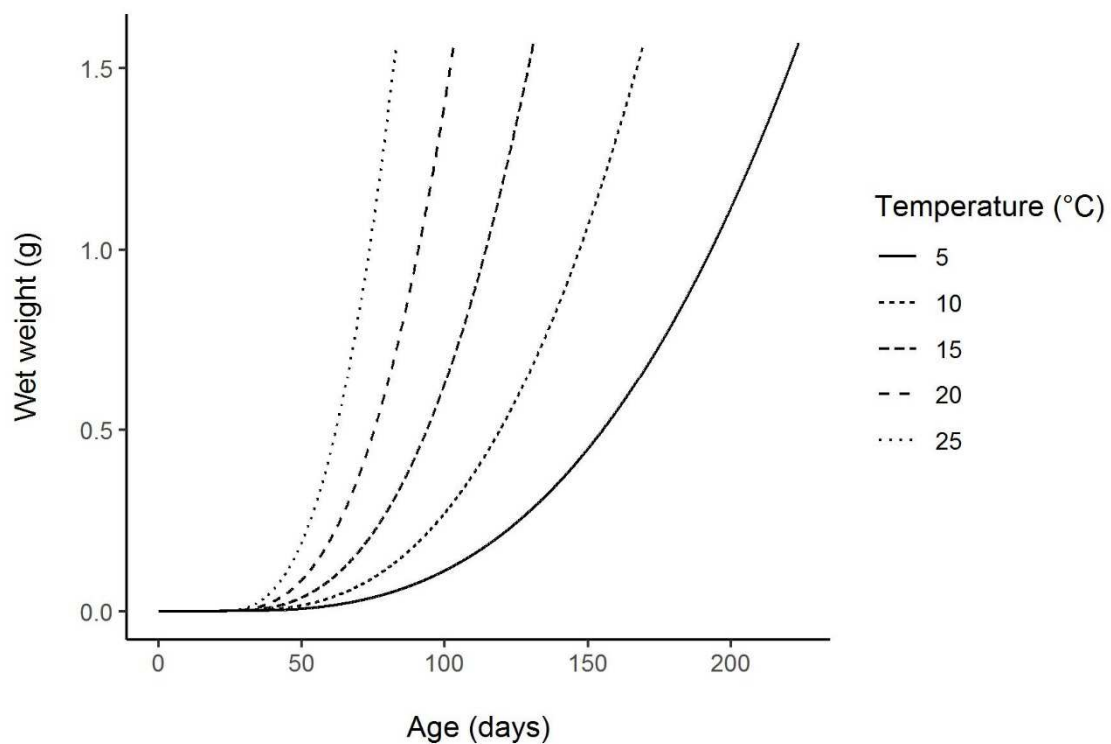
706

707 Figure 6. DEB simulations of *H. diversicolor* individual growth in L3 length (cm) and
708 wet weight (WW) (g) with temperatures ranging from 5°C to 25°C. Simulations were
709 performed until the maximum observed size (1.57 g, Add my Pet database, Lefebvre,
710 2019) (based on the literature) was reached. The functional scaled response was
711 maintained constant at $f=1$.

712 a)



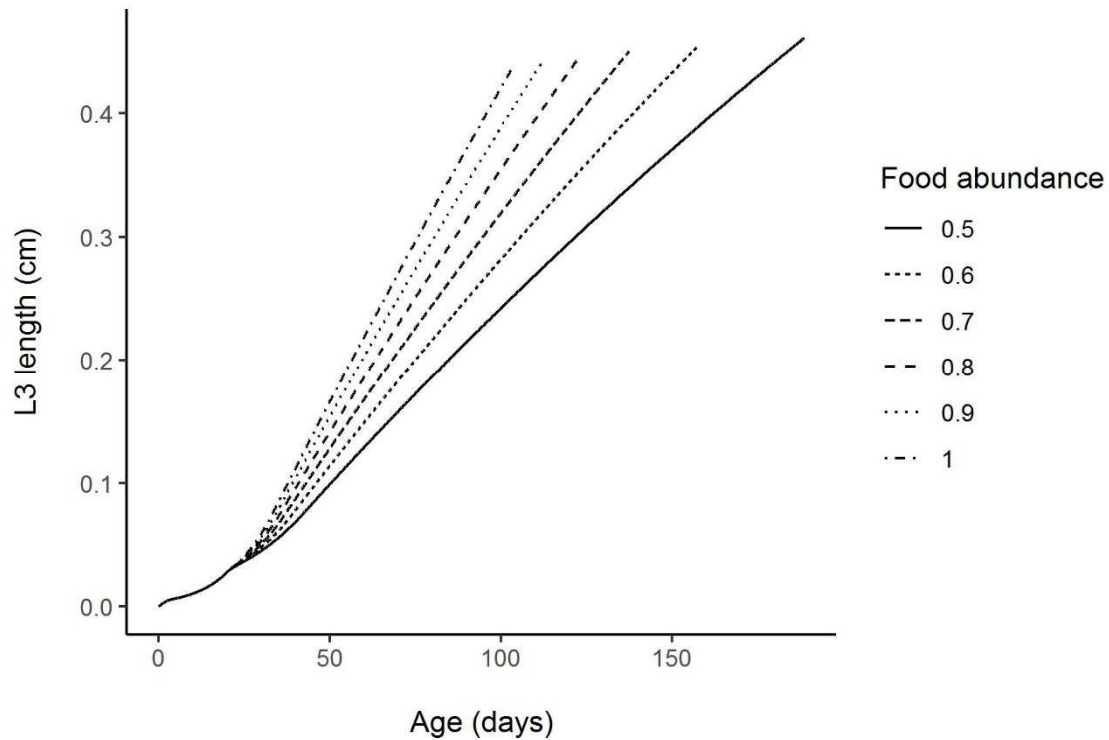
713 b)
714



715

716 Figure 7. DEB simulations of *H. diversicolor* individual growth in a) L3 length (cm)
 717 and b) wet weight (WW) (g) over time (days) according to different food abundance
 718 (scaled functional response, f) scenarios. Simulations were performed until the GSI for
 719 first reproduction was reached (3%). The temperature was maintained constant at 20°C.
 720 f at 0.5 means that individuals were fed at 50% of *ad libitum*.

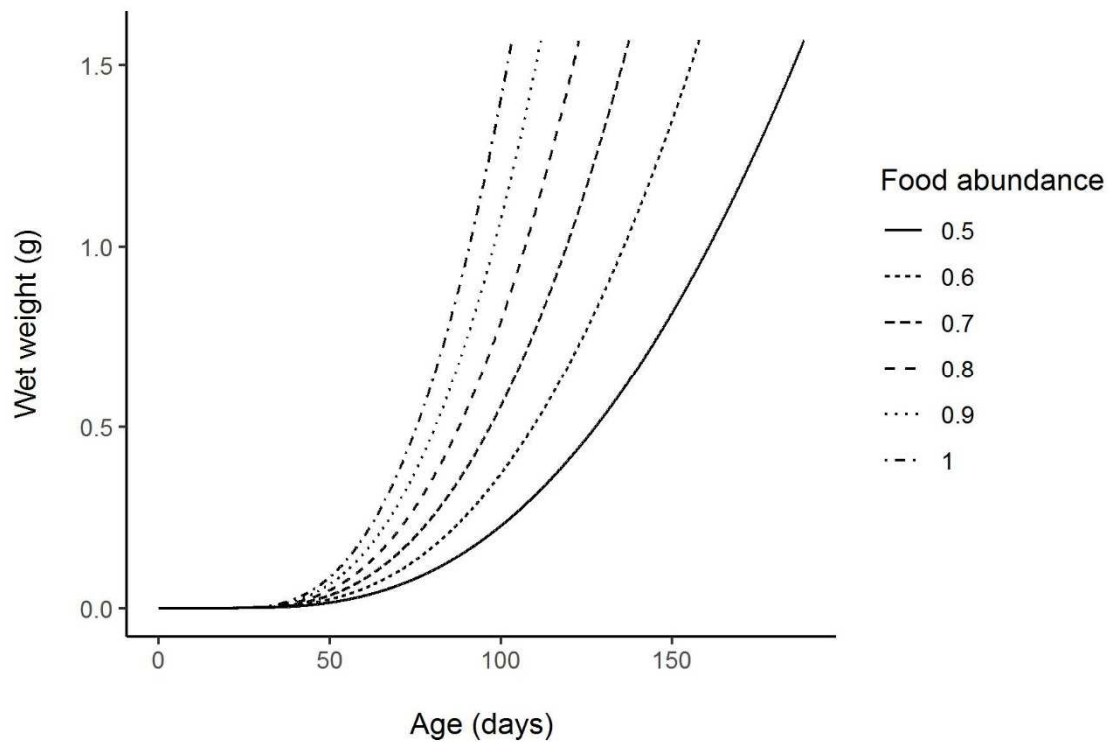
721 a)



722

723

b)



724

725

726

727 Table 1. DEB abj-model parameters estimated for the polychaete *Hediste diversicolor*
 728 (Lefebvre, 2019, Add-my-Pet database).

729

Parameters	Value	Unit	Description
L_m	0.53073	Cm	Maximum volumetric length
$\{\dot{p}_{Am}\}$	14.3197	J cm ⁻² d ⁻¹	Maximum surface-specific assimilation rate
\dot{v}	0.01123	cm d ⁻¹	Energy conductance (velocity)
g	2.761754	-	Energy investment ratio
\dot{k}_J	0.002	d ⁻¹	Maturity maintenance rate coefficient
\dot{k}_M	0.007663691	d ⁻¹	Somatic maintenance rate
κ	0.96018	-	Allocation fraction to soma
κ_R	0.95	-	Reproduction efficiency
$[\dot{p}_M]$	25.91	J cm ⁻³ d ⁻¹	Volume specific somatic maintenance rate
$[E_G]$	3380.46	J cm ⁻³	Volume specific costs of structure
E_H^b	0.0003164	J	Energy maturity at birth
E_H^j	0.7665	J	Energy maturity at metamorphosis
E_H^p	7.883	J	Energy maturity at puberty
T_A	4877.15	K	Arrhenius temperature
T_{ref}	293.15	K	Reference temperature
ω	0.440695	-	Contribution of reserve to body weight or physical volume
δ_M	2.3579	-	Shape coefficient for L3 length
η_{OA}	0.329	$\mu\text{mol-O}_2 \text{ J}^{-1} \text{ d}^{-1}$	Energy-oxygen coupling coefficient for the assimilation flux
η_{OD}	1.977	$\mu\text{mol-O}_2 \text{ J}^{-1} \text{ d}^{-1}$	Energy-oxygen coupling coefficient for the dissipation flux
η_{OG}	0.285	$\mu\text{mol-O}_2 \text{ J}^{-1} \text{ d}^{-1}$	Energy-oxygen coupling coefficient for the growth flux
η_{NA}	0.045	$\mu\text{mol-NH}_3 \text{ J}^{-1} \text{ d}^{-1}$	Energy-ammonia coupling coefficient for the assimilation flux
η_{ND}	0.273	$\mu\text{mol-NH}_3 \text{ J}^{-1} \text{ d}^{-1}$	Energy-ammonia coupling coefficient for the dissipation flux
η_{NG}	0.039	$\mu\text{mol-NH}_3 \text{ J}^{-1} \text{ d}^{-1}$	Energy-ammonia coupling coefficient for the growth flux

730

731

732

733 Table 2. Growth performance of *Hediste diversicolor* fed with fish faeces and
 734 commercial fish feed over time (age in days), and associated means of L3 length (cm),
 735 wet weight (WW g) and survival: n = number of observations and SD = standard
 736 deviation. Statistical analysis was performed with food type as fixed factor and tank as
 737 random factor (* when $p < 0.05$).
 738

Age (days)	Food type	n	L3 \pm SD (cm)	WW \pm SD (g)	Survival (%)
113	Fish faeces	54	0.11 \pm 0.02		
	Fish feed	54	0.12 \pm 0.02		
144	Fish faeces	50	0.21 \pm 0.05		93
	Fish feed	52	0.18 \pm 0.05		96
177	Fish faeces	45	0.30 \pm 0.05*	0.35 \pm 0.16	83
	Fish feed	42	0.27 \pm 0.05*	0.30 \pm 0.18	78
211	Fish faeces	31	0.30 \pm 0.05	0.41 \pm 0.17	57
	Fish feed	26	0.28 \pm 0.06	0.36 \pm 0.15	48

739
 740
 741

742 Table 3. Effects of temperature and scaled functional response ($f=0.5$, $f=0.6$ and $f=1$ at
 743 20°C ; 5°C and 25°C with $f=1$) on *H. diversicolor* L3 length (cm), wet weight (WW g)
 744 and total assimilated energy (Assim in J) and faeces assimilation (g DW). Total
 745 assimilated energy was estimated over ragworm production cycle (see Wang et al. 2020
 746 for production cycle description). A production cycle was stopped when GSI reached
 747 3%, or when WW reached 0.5 g WW (minimum polychaete market weight). The
 748 bioremediation capacity of one individual was estimated by transforming the
 749 assimilated energy in fish faeces by assuming (based on the literature) that 1 g of fish
 750 faeces represents 10.4 kJ. A population density of 3700 ind.m⁻² (Scaps, 2002) was
 751 chosen to estimate the bioremediation capacity of a ragworm farm per m² and year.
 752
 753

T (°C)	f	age days	L3 cm	WW g	GSI %	Surv %	Assim (per ind.)			Bioremediation	
							J cycle ⁻¹	J yr ⁻¹	g (DW) yr ⁻¹	g (DW) m ⁻² yr ⁻¹	kg (DW) 100m ⁻² yr ⁻¹
up to 3% GSI											
20	0.5	99	0.24	0.2	3.0	90	641	2370	0.23	755	75
20	1	79	0.31	0.6	3.0	90	1603	7443	0.72	2370	237
5	1	163	0.31	0.6	3.0	90	1596	3572	0.34	1137	114
25	1	64	0.31	0.6	3.0	90	1600	9067	0.87	2887	289
up to 0.5 g WW											
20	0.5	128	0.32	0.5	3.9	67	1536	4390	0.42	1039	104
20	1	75	0.30	0.5	2.9	90	1363	6598	0.63	2122	212
5	1	155	0.30	0.5	2.9	90	1355	3187	0.31	1025	103
25	1	62	0.30	0.5	2.9	90	1362	8020	0.77	2579	258

754